Supporting Information

Metallic P_3C Monolayer as Anode for Sodium-ion Batteries

Ziyuan Zhao, ‡ Tong Yu, ‡ Shoutao Zhang, Haiyang Xu*, Guochun Yang* and Yichun Liu

Centre for Advanced Optoelectronic Functional Materials Research and Laboratory for UV Light-Emitting Materials and Technology of Ministry of Education, Northeast Normal University, Changchun 130024, China.

*Address correspondence to: yanggc468@nenu.edu.cn

Index **page**

Computational Details

The particle swarm optimization (PSO) method within the evolutionary algorithm as implemented in the Crystal structure AnaLYsis by Particle Swarm Optimization (CALYPSO) code[1-2] was employed to find the lowest energy structures of P_xC_y (x = 1 – 8 and y = 1; x = 1 and y = 1 – 8; x = 3 and y = 2; x = 2 and y = 3) monolayers. Unit cells containing 1, 2, and 4 formula units (f.u.) were considered. In the first step, random structures with certain symmetry are constructed in which atomic coordinates are generated by the crystallographic symmetry operations. Local optimizations using the VASP code[3] were done with the conjugate gradients method and stopped when Gibbs free energy changes became smaller than 1×10^{-5} eV per cell. After processing the first generation structures, 60% of them with lower Gibbs free energies are selected to construct the next generation structures by PSO. 40% of the structures in the new generation are randomly generated. A structure fingerprinting technique of bond characterization matrix is applied to the generated structures, so that identical structures are strictly forbidden. These procedures significantly enhance the diversity of the structures, which is crucial for structural global search efficiency. In most cases, structural searching simulations for each calculation were stopped after generating 1000 ~ 1200 structures (e.g., about 20 ~ 30 generations).

The local structural relaxations and electronic properties calculations were performed in the framework of the density functional theory (DFT)[4] within the generalized gradient approximation (GGA)[5] parametrized as implemented in the VASP code. The $3s^23p^3$, $2s^22p^2$, and $3s^1$ atomic orbitals were treated as valence states for P, C, and Na, respectively. The cut-off energy for the expansion of wave functions into plane waves was set to 700 eV in all calculations. According to the Monkhorst-Pack scheme,[6] a $8 \times 12 \times 1$ Γ-centered k-point meshes were selected for the structural optimization and electronic properties calculations, and a $4 \times 6 \times 2$ k-point grids were used during the sodiation process.

We found a dynamic and thermal stable P_3C monolayer through first principles swarm structural search. Phonon dispersion calculations were performed for 2×3 supercell for P_3C, which was based on supercell approach as done in the Phonopy code.[7] First-principles molecular dynamics (MD)[8] simulations for large 2×3 P_3C supercell were performed at temperature of 1000 K. MD simulation in NVT ensemble lasted for 10 ps with a time step of 1.0 fs. The temperature was controlled by using the Nosé-Hoover method.

Supporting Figures

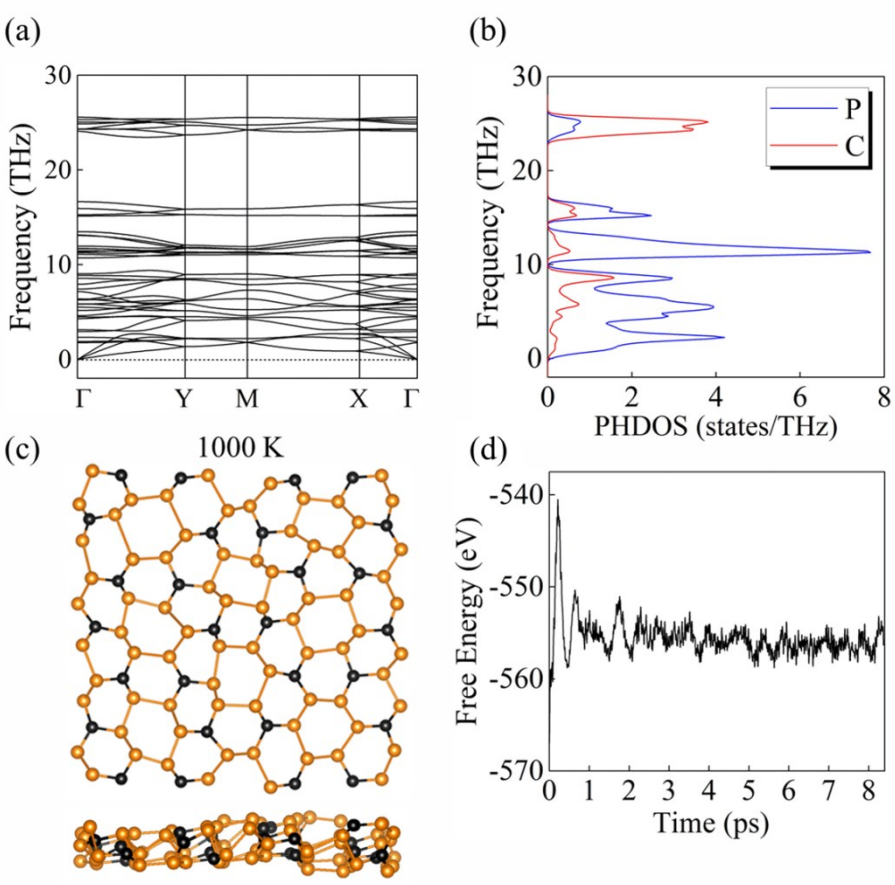

Figure S1. Phonon spectra and thermal stability of C_2/m P_3C monolayer. (a) Phonon dispersive curves and (b) projected phonon density of states (PHDOS) of P_3C. (c) Snapshots after equilibration and (d) free energy as a function of MD time of the final frame of P_3C monolayer at temperatures of 1000 K at the end of 10 ps MD simulations.

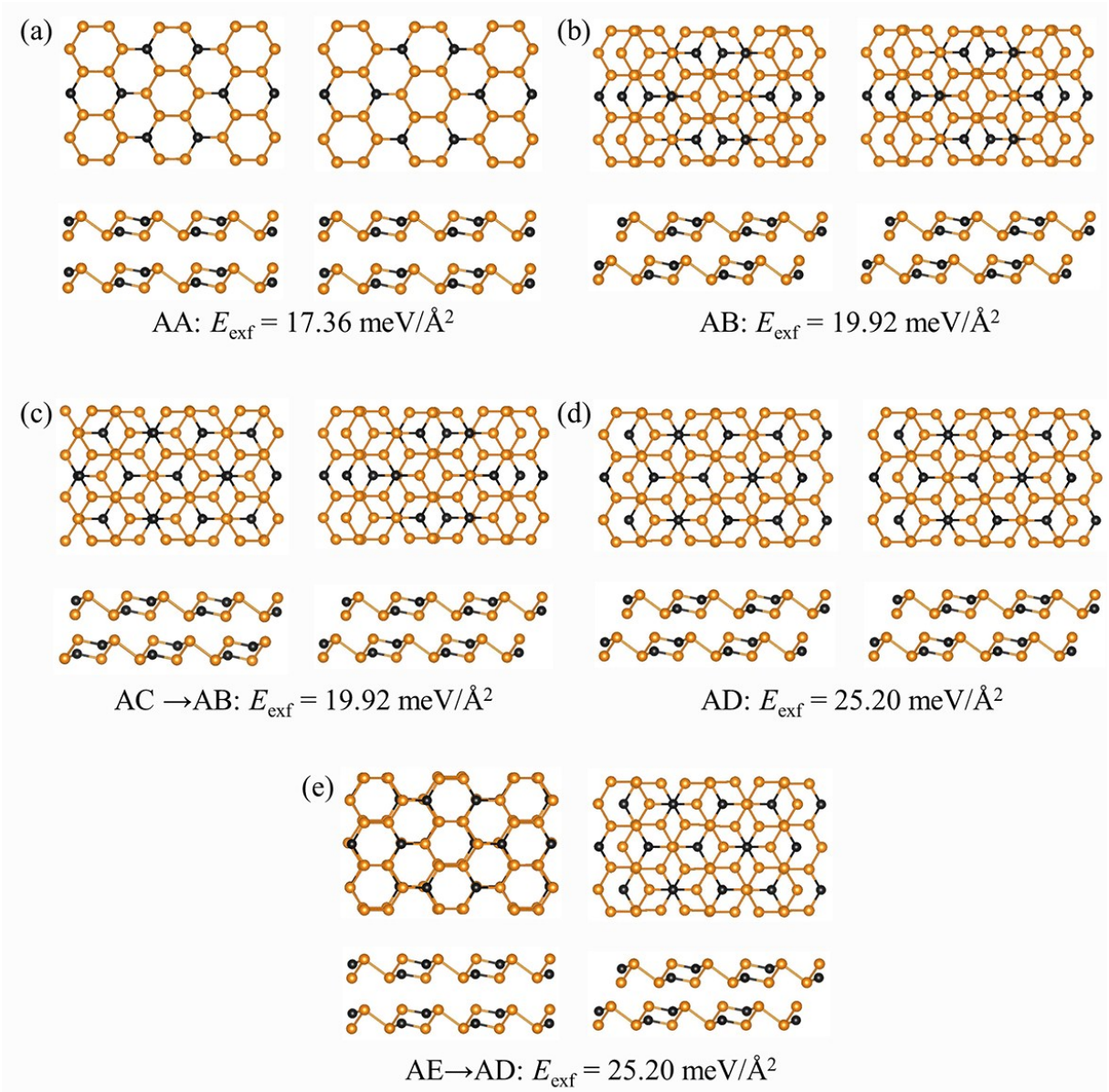

Figure S2. Calculated initial (left), optimized (right) structures and corresponding exfoliation energy (E_{exf}) of five possible stacking patterns of P_3C bilayer. After fully geometry relaxation, AC stacking pattern transforms to AB stacking pattern and AE stacking pattern transforms to AD stacking pattern. The most stable double-layer P_3C is AD stacking pattern.

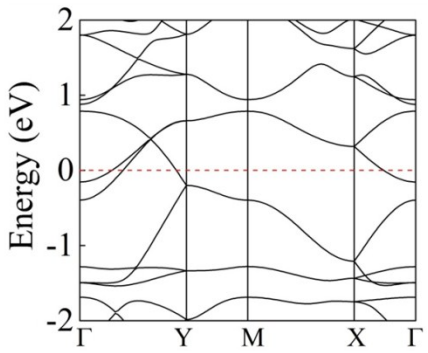

Figure S3. Electronic band structures of P_3C monolayer.

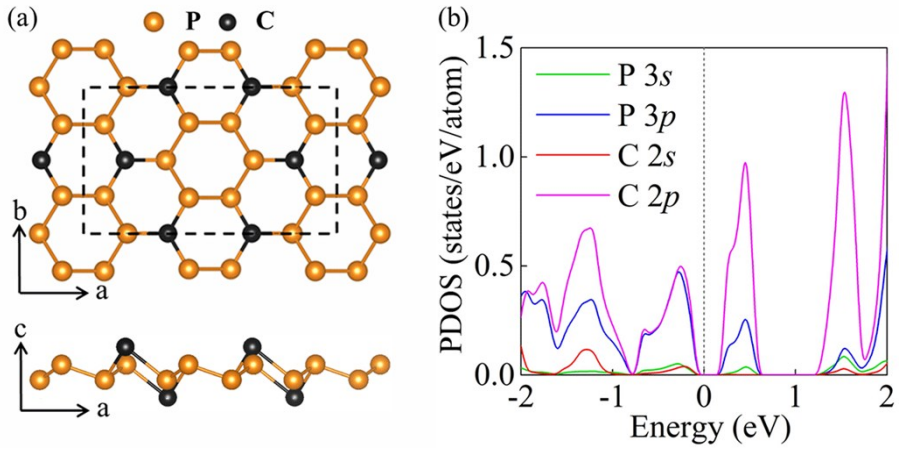

Figure S5. (a) GeP_3-structure P_3C monolayer and (b) its projected density of states (PDOS).

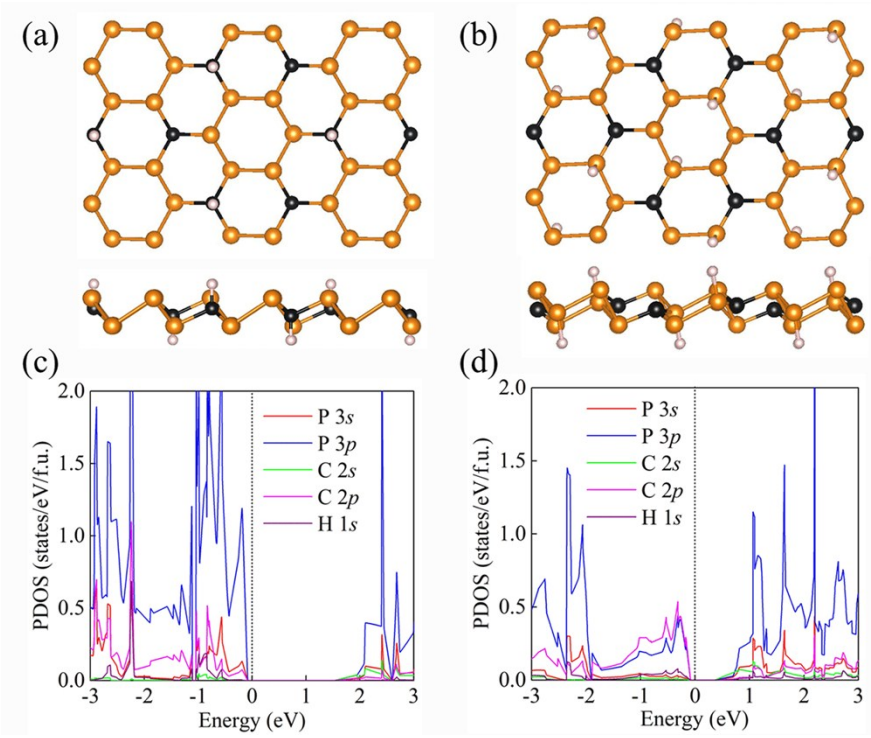

Figure S4. We performed hydrogenation on P_3C monolayer, hydrogenated at C or P atom are labeled P_3CH or HP_3C. Optimized structure of P_3CH (a) and HP_3C (b). The PDOS of P_3CH (c) and HP_3C (d) have been calculated along with orbital projection for p and s orbitals of C and P and the s orbital of H. The dashed line is the Fermi level. For HP_3C, due to P_3C cannot accommodate more H atoms for full hydrogenation at P atoms, we selected a couple of P sites to adsorb H atoms.

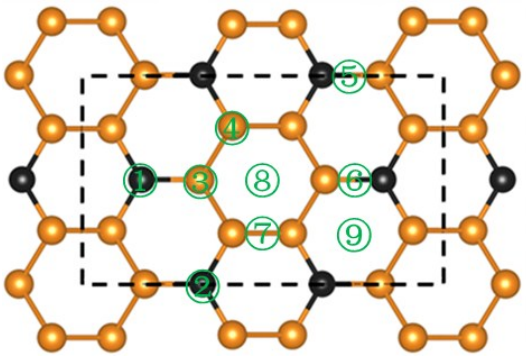

Figure S6. Top view of the representative adsorption sites on the P_3C monolayer. 1, 2, 3 and 4 are on the top of different C and P atoms. 5, 6 and 7 are on the top of bridge sites. 8 and 9 are on the top of hollow sites.

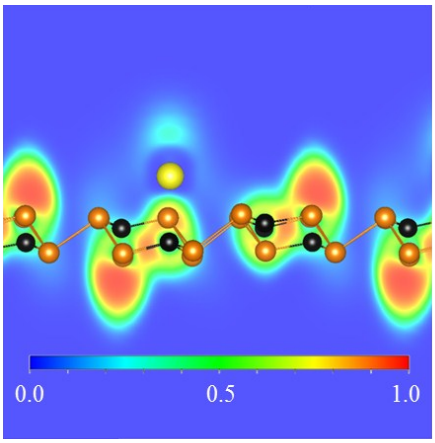

Figure S7. ELF map of P_3C monolayer absorbing one Na-ion.

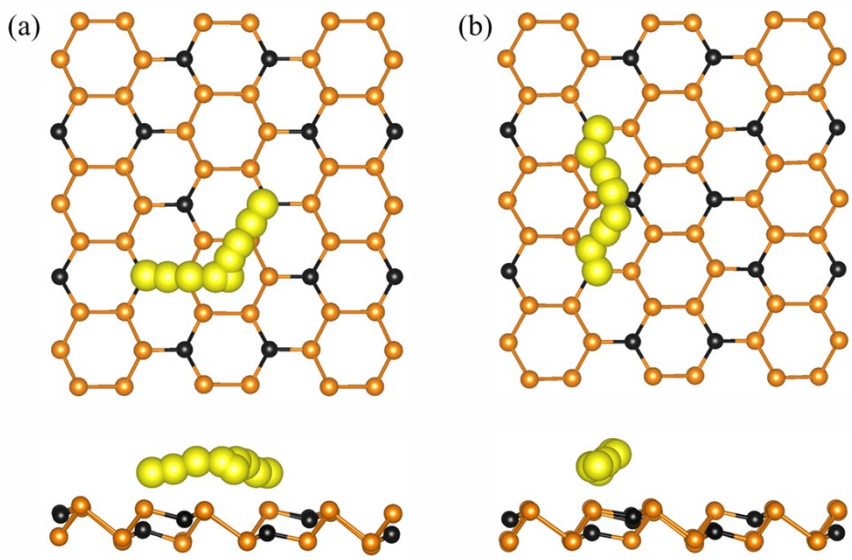

Figure S8. The diffusion trails of Na ion on P_3C monolayer for Path I (a) and Path II (b). The diffusion length of Path I is 7.30 Å and for Path II is 7.09 Å.

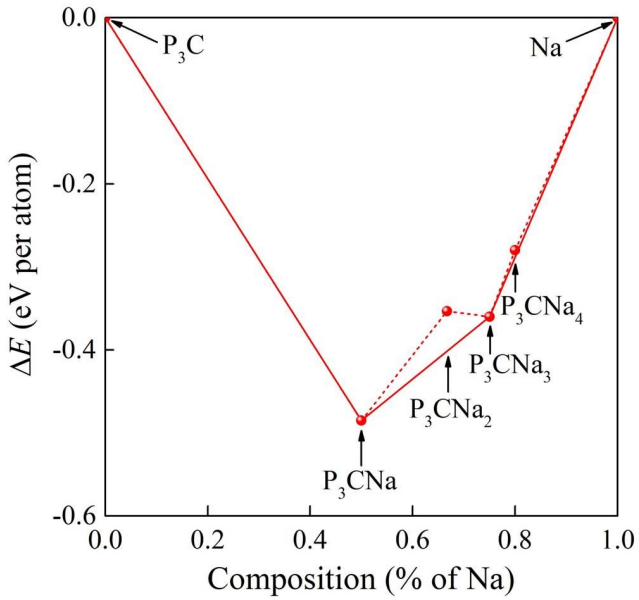

Figure S9. Relative stabilities of P_3CNa_n (n = 1−4) with respect to an elemental solid Na and P_3C monolayer at 0 K.

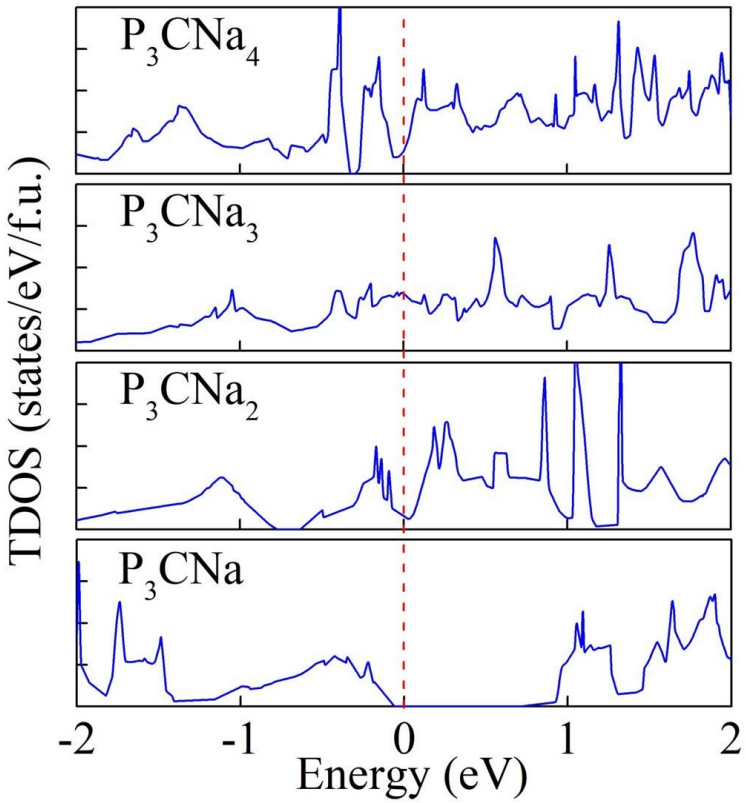

Figure S10. Total projected density of states (TDOS) of P_3CNa, P_3CNa_2, P_3CNa_3 and P_3CNa_4.

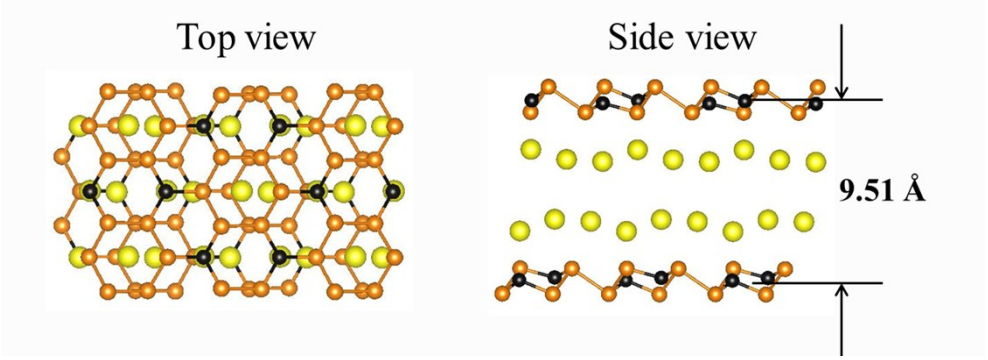

Figure S11. Optimized geometry of P_3C bilayer with two-layer intercalated Na atoms within layers. The interlayer distance is 9.51 Å.

Supporting Table

Table S1. Structural information of the predicted P_3C monolayer.

Phase	Space Group	Lattice Parameters (Å, °)	Wyckoff Positions (fractional)			
			Atoms	*x*	*y*	*z*
P_3C	*C*2/*m*	a = 10.79480	P(8j)	0.91692	0.74315	0.53358
		b = 6.23410	P(4i)	0.17370	0.00000	0.53354
		c = 19.93480	C(4i)	0.66540	0.00000	0.48325
		$\alpha = \gamma$ = 90.00000				
		β = 92.32730				

References

(1) Wang, Y.; Lv, J.; Zhu, L.; Ma, Y. Crystal structure prediction via particle-swarm optimization. *Phys. Rev. B* **2010,** *82*, 094116.

(2) Wang, Y.; Lv, J.; Zhu, L.; Ma, Y. CALYPSO: A method for crystal structure prediction. *Comput. Phys. Commun.* **2012,** *183*, 2063-2070.

(3) Kresse, G.; Furthmüller, J. Efficient iterative schemes for ab initio total-energy calculations using a plane-wave basis set. *Phys. Rev. B* **1996,** *54*, 11169.

(4) Kohn, W.; Sham, L. J. Self-consistent equations including exchange and correlation effects. *Phys. Rev.* **1965,** *140*, A1133.

(5) Perdew, J. P.; Burke, K.; Ernzerhof, M. Generalized gradient approximation made simple. *Phys. Rev. Lett.* **1996,** *77*, 3865.

(6) Monkhorst, H. J.; Pack, J. D. Special points for Brillouin-zone integrations. *Phys. Rev. B* **1976,** *13*, 5188.

(7) Togo, A.; Oba, F.; Tanaka, I. First-principles calculations of the ferroelastic transition between rutile-type and $CaCl_2$-type SiO_2 at high pressures. *Phys. Rev. B* **2008,** *78*, 134106.

(8) Martyna, G. J.; Klein, M. L.; Tuckerman, M. Nosé–Hoover chains: the canonical ensemble via continuous dynamics. *J. Chem. Phys.* **1992,** *97*, 2635-2643.